

THE IMPORTANCE OF TIME-DEPENDENT FLAME STRUCTURES IN STRETCHED LAMINAR FLAMELET MODELS FOR TURBULENT JET DIFFUSION FLAMES

D. C. HAWORTH¹, M. C. DRAKE¹, S. B. POPE² AND R. J. BLINT¹

¹General Motors Research Laboratories
Warren, Michigan 48090

²Sibley School of Mechanical & Aerospace Engineering
Cornell University
Ithaca, New York 14853

The stretched laminar flamelet model provides a convenient mechanism for incorporating realistic chemical kinetics into calculations of turbulent nonpremixed flames. In the standard flamelet model, two scalars, a mixture fraction ξ and scalar dissipation χ (a measure of flamelet stretch) suffice to specify the local instantaneous thermochemical state in the turbulent flow. One shortcoming of the flamelet approach is the implicit assumption that the reaction zone structure of laminar flamelets can respond on a time scale that is fast compared to the time scale of changes in mean scalar dissipation in the turbulent flow. Analysis of the response of a one-dimensional unsteady strained diffusion layer to arbitrary time-dependent strains is presented. This analysis suggests that laminar flames cannot approach the equilibrium (zero strain) structure as rapidly as the flamelet model implies far downstream in the jet; the flamelet model breaks down in the far jet. An ad hoc modification to the flamelet model is made to account for the limited response of the diffusive layer to time-varying strain rates. In a CO/H₂/N₂-air turbulent jet diffusion flame, the modified flamelet model yields a substantially slower approach to chemical equilibrium and improved agreement with experimental data compared to the standard flamelet model. This suggests that the final approach to equilibrium may be limited by the nonzero response time of flamelet chemical structure to the rapidly decaying strain rates encountered downstream in the turbulent jet. In the context of flamelet models, transient effects may be more important than previously assumed.

Introduction

Turbulent nonpremixed flames of practical importance often exhibit significant departures from chemical equilibrium through phenomena such as superequilibrium radical formation, pollutant formation, extinction, and sooting. One approach to including these effects in turbulent flow calculations is the laminar flamelet model.^{1,2,3} Here, the local instantaneous structure of the reaction zone in the turbulent flow is assumed to be the same as that in a quasi-steady one-dimensional laminar flame, albeit convected and distorted by the turbulent velocity field. In the standard flamelet model, the principal influence of turbulence on the chemical structure of the laminar flame is through the amount of stretching that the flame is subjected to by the turbulent flow field; the amount of stretch is quantified by the scalar dissipation rate. Thus two scalars, the mixture fraction or normalized fuel mass fraction ξ and scalar dissipation χ , suffice to de-

scribe the instantaneous thermochemical state in the turbulent flow.

Several flamelet-based modeling studies of turbulent jet diffusion flames have been reported.^{4,5,6} Although reasonable agreement between model calculations and experimental results has been claimed, the comparisons have been limited by the lack of measurements of variables (such as OH concentrations) that are very sensitive to the chemistry model and by the existence of extensive extinction and premixing effects. In a recent paper,⁷ the standard flamelet model has been applied to the CO/H₂/N₂-air jet that is the subject of the present modeling study.^{8,9,10} This flame exhibits strong non-equilibrium effects without the complication of local extinction and premixing; the principal discrepancy between the model results and experiment is the model's overly rapid decay of OH superequilibrium with distance downstream of the nozzle.

One shortcoming of the standard flamelet theory is the implicit assumption that the laminar flame

structure can remain in quasi-equilibrium with the local scalar dissipation rate encountered in the turbulent flow. The present analysis suggests that the residence time of a flamelet in the turbulent jet imposes a limit on the steady-state flame structure that can be realized in response to a time-varying turbulent strain field. Experiments¹¹ in laminar opposed-flow diffusion flames with sinusoidally varying stretch show that the time response of the flame structure can be long and is inversely related to the stretch.

The purpose of this paper is to present an ad hoc modification to the standard flamelet approach that accounts for the nonzero response time of flamelets. The basis for the modification is the equivalent strain model developed below. Turbulence closure is at the level of the one-point joint probability density function (pdf) of the velocities, mixture fraction, and scalar dissipation; the modeled pdf transport equation is solved numerically using a Monte Carlo method.¹²

Turbulent Jet Diffusion Flame

The subject of this study is a syngas-air turbulent jet diffusion flame.^{8,9,10} Fuel (40% CO, 30% H₂, 30% N₂ molar) exits from a nozzle of diameter $D = 3.18$ mm with an average velocity of $\bar{U}_D = 54.6$ m/s into a coflowing air stream that is moving with speed $U_E = 2.4$ m/s. The nozzle Reynolds number $Re_D = \bar{U}_D D / \nu$ is 8500. Simultaneous measurements of density, temperature, and major species concentrations (H₂, O₂, N₂, CO, and H₂O) have been made using pulsed Raman scattering at axial stations $x/D = 10, 25,$ and 50 .⁸ From these measurements are inferred the CO₂ concentration and the mixture fraction, ξ . Laser saturated fluorescence has been used to measure OH concentration.⁹ A comparison of results from the standard flamelet model with results from three earlier modeling studies of this flow using different chemistry models and different levels of turbulence closures may be found in Haworth et al.⁷

Stretched Laminar Flamelet Model

The application of a flamelet model to turbulent diffusion flames was proposed by Carrier et al.¹ and Williams,² and has been developed by Peters,³ Liew et al.,⁴ and others.⁵ For a fixed value of scalar dissipation, all thermochemical properties are related to the value of a single conserved scalar mixture fraction ξ that varies from $\xi = 0$ (pure air) to $\xi = 1$ (pure fuel) through the laminar flamelet. The

variable that characterizes the distortion of a flamelet by the turbulent flow is the scalar dissipation χ ,

$$\chi \equiv 2\Gamma \frac{\partial \xi}{\partial x_i} \frac{\partial \xi}{\partial x_i} \quad (1)$$

Here Γ is the molecular diffusivity of the mixture and the usual summation convention over repeated indices applies. Although χ varies through the laminar flame, it is convenient to choose a single value of scalar dissipation to characterize each flamelet. We use the value of the scalar dissipation at the stoichiometric mixture fraction $\chi_{St} \equiv \chi|_{\xi=\xi_{St}}$. Choosing χ at the peak temperature or choosing the actual calculated value of χ for each ξ through the flamelet is not expected to change significantly the turbulent combustion calculations. For the CO/H₂/N₂-air system, $\xi_{St} \approx 0.3$.

A library of 17 flamelets for 17 different values of χ_{St} has been generated for the CO/H₂/N₂-air flame^{13,14} for values of scalar dissipation from $\chi_{St} = 0$ (chemical equilibrium) to $\chi_{St} = \chi_q = 1380.7/s$ (extinction limit); this corresponds to values of stretch ($\alpha = 0$ to $\alpha_q = 4800/s$). These laminar diffusion flame calculations are performed for an opposed-flow stagnation point burner configuration using a kinetics scheme that includes 15 species and 32 reactions; realistic molecular transport properties (e.g., differential diffusion) are included. There is good agreement between these calculations and measurements in CO/H₂/N₂-air laminar opposed-flow diffusion flames.¹³

A discussion of the appropriateness of flamelet models for the CO/H₂/N₂-air jet has been given by Haworth et al.⁷ Laminar flame thicknesses for this flame typically are larger than the smallest turbulence mixing scales so that turbulence probably does modify the laminar flame structure. We expect, then, that the flamelet model cannot be quantitatively correct for this flame. However, the flamelet model is the only turbulent combustion model that includes the physically important coupling between chemical reaction and molecular diffusion; we believe that the flamelet model is useful in understanding the importance of this interaction. In the analysis and computations that follow, it is suggested that the time dependency of flame structures may be more important than previously assumed in the flamelet approach. By taking account of this transient effect in a simply way, significant improvements over the results of the standard flamelet model are realized.

Equivalent Strain Model

We consider the following simplified model for a strained laminar flamelet: a one-dimensional un-

steady strained diffusive layer described by a scalar function $c(x,t)$ (a normalized concentration, say) is subjected to a time-dependent strain rate $a(t)$; the constant diffusion coefficient is D . Then $c(x,t)$ is governed by the one-dimensional unsteady convection-diffusion equation,

$$\frac{\partial c}{\partial t} - a(t)x \frac{\partial c}{\partial x} = D \frac{\partial^2 c}{\partial x^2}. \quad (2)$$

Initial and boundary conditions are

$$c(x,t_0) = H(x), \quad c(-\infty,t) = 0, \quad c(\infty,t) = 1, \quad (3)$$

where $H(x)$ is the Heaviside function.

A self-similar solution exists for this problem. Transformed space and time coordinates and scalar function are defined by

$$y = x/w(t), \quad \tau = t, \quad b(y,\tau) = c(x,t), \quad (4)$$

where $w(t) > 0$ is a function to be specified. If $w(t)$ satisfies the ordinary differential equation

$$\frac{d(w^2/2)}{dt} + a(t)w^2 = D, \quad (5)$$

with initial condition $w(t_0) = 0$, then Eq. (2) admits a stationary error function solution,

$$\begin{aligned} b(y,\tau) = b(y) &= (2\pi)^{-1/2} \int_{-\infty}^y \exp\{-z^2/2\} dz \\ &= [1 + \operatorname{erf}(y/\sqrt{2})]/2. \end{aligned} \quad (6)$$

The solution to Eq. (5) is

$$w^2(t) = 2D \int_{t_0}^t \exp\left\{-2 \int_{t'}^t a(t'') dt''\right\} dt'. \quad (7)$$

Thus for an arbitrary strain-rate history $a(t)$, the profile $c(x,t)$ is a self-similar error function with width $w(t)$ given by Eq. (7).

If a steady strain rate A is applied, Eqs. (5) and (7) show that, asymptotically at large time, the width is $w = (D/A)^{1/2}$. Equating this expression to the right-hand side of Eq. (7) gives an equivalent quasi-steady strain rate A that yields the same $c(x)$ profile as the actual strain history $a(t)$. The equivalent quasi-steady strain rate is given by

$$A^{-1}(t) = 2 \int_{t_0}^t \exp\left\{-2 \int_{t'}^t a(t'') dt''\right\} dt'. \quad (8)$$

This quantity satisfies the simple ordinary differential equation

$$\frac{dA}{dt} = -2A^2(t) + 2a(t)A(t). \quad (9)$$

Now consider the implications of these results for the turbulent jet diffusion flame. If the strain history $a(t)$ following a flamelet (a strained diffusive layer, by assumption) were known, then Eq. (9) could be integrated to find the equivalent quasi-steady strain appropriate for each flamelet. However, the strain rate is not available in most modeling approaches to turbulent flows, including the present one-point joint pdf closure. A simpler approach is sought.

Some motivation for a simpler model is provided by scaling arguments. In the transient laminar diffusion layer, it takes a time of the order of the residence time of a fluid particle for the steady-state profile to establish itself following a perturbation in strain rate. Thus in the turbulent jet, we expect that $A(t)$ can decrease no faster than linearly with the residence time of a particle in the flow.

The same conclusion can be deduced from Eq. (9). The inverse strain rate a^{-1} is of the order of the Kolmogorov time scale τ_k ; dimensional reasoning in a self-similar turbulent axisymmetric jet shows that τ_k scales as $(x/D)^2$.¹⁵ The differential equation $dA/dt = -2A^2$ (Eq. 9 without the final term on the right-hand side) has the exact solution

$$A(t) = \frac{A_0}{2A_0(t - t_0) + 1}, \quad (10)$$

where $A_0 \equiv A(0)$. Thus the first term on the right-hand side of Eq. (9) causes $A(t)$ to decay as $(x/D)^{-1}$. For $A_0 > 0$ then, Eq. (10) can be interpreted as a lower bound on the equivalent strain rate since the term in Eq. (9) containing $a(t)$ becomes unimportant for large x/D . In the turbulent flow, we implement this idea by replacing flamelets with values of stretch less than $\alpha_{\min} = A(t)$ (Eq. 10) by a flamelet with $\alpha = \alpha_{\min}$. This does not imply that lower values of stretch do not exist in the turbulent flow, but only that laminar flamelets cannot adjust rapidly enough to have a steady-state structure corresponding to such low values of stretch.

The result of Eq. (9) is contained in the standard flamelet theory: there is a one-to-one correspondence between $A(t)$ and the local scalar dissipation rate χ_3 at any point through the diffusive layer. Peters³ shows that the laminar flame structure in the turbulent flow is quasi-steady when expressed in terms of scalar dissipation; the dependence on the time-varying strain field is implicit. Here we revert to strain rate so that the response of flame

structure to time-varying strain rates is explicitly in evidence.

Three points can be made concerning the use of scalar dissipation vs. strain rate in laminar flamelet models for turbulent diffusion flames. First, for a turbulent flow where the mixture fraction ξ varies from zero to unity across the flame (e.g., a turbulent mixing layer), the standard flamelet model expressed in terms of scalar dissipation contains the same time dependency of flame structure as the above transient diffusion layer analysis. Second, for flows such as turbulent jets where mixing outside of the reaction zone leads to a negligible probability of encountering pure fuel far downstream (i.e., ξ varies between zero and some value less than unity across flamelets), the relationship between thermochemical properties and mixture fraction in flamelets with modified ξ boundary conditions is the same as in zero-to-unity flamelets at the same χ . In the strain rate approach, the changing boundary conditions on mixture fraction should be accounted for in some way. And third, the time-dependent analysis presented here shows that for an isolated zero-to-one mixture fraction flamelet, the residence time in the flow sets a lower limit on the equivalent quasi-steady strain rate. The standard flamelet model implies the existence of flames that are too "old," i.e., too close to chemical equilibrium, far downstream. This is another manifestation of the breakdown of the flamelet model far downstream in the jet. The question then arises of how to specify thermochemical properties in the turbulent flame. The approximation adopted here (without complete physical justification) is to continue to use steady-state laminar flame properties, but with a lower bound on flamelet scalar dissipation imposed by the residence time of the flamelet in the flow. This biases the flamelet distribution towards "newer" flames further from chemical equilibrium downstream in the jet.

Turbulent Flow Models

Turbulence closure is at the level of the one-point joint probability density function of the velocities $\mathbf{U}(\mathbf{x}, t)$ and of the scalars describing the thermochemical state of the system, $\xi(\mathbf{x}, t)$ and $\chi(\mathbf{x}, t)$. Because the flow is statistically stationary and axisymmetric, one-point statistics are functions of axial coordinate x and of radial coordinate r only. The velocity-composition joint pdf $\tilde{f}_{\mathbf{U}\xi\chi}(\mathbf{V}, \hat{\xi}, \hat{\chi}; x, r)$ is the density-weighted probability density of the event $\{\mathbf{U}(\mathbf{x}, t) = \mathbf{V}, \xi(\mathbf{x}, t) = \hat{\xi}, \chi(\mathbf{x}, t) = \hat{\chi}\}$. All one-point statistics of any function of the velocities and compositions can be determined from $\tilde{f}_{\mathbf{U}\xi\chi}$. For example, the density-weighted mean mixture fraction $\bar{\xi}(x, r)$ is given by

$$\bar{\xi}(x, r) = \iiint \hat{\xi} \tilde{f}_{\mathbf{U}\xi\chi}(\mathbf{V}, \hat{\xi}, \hat{\chi}; x, r) d\mathbf{V} d\hat{\xi} d\hat{\chi}, \quad (11)$$

where the integration is over the entire velocity-composition space. A tilde denotes a density-weighted or Favre-averaged mean.

A transport equation for the joint pdf can be derived from the governing Eulerian conservation equations for the flow.¹² The effects of strongly nonlinear reaction source terms, the mean pressure gradient, and convective transport appear in closed form in the evolution equation for the one-point velocity-composition joint pdf; the processes to be modeled are molecular transport and the fluctuating pressure gradient.

In the turbulent jet, it is assumed that the scalar dissipation is statistically independent of the velocities and mixture fraction.^{4,5,6,7} The marginal pdf of scalar dissipation $\tilde{f}_{\chi}(\hat{\chi}; x, r)$ can then be isolated from the velocity-mixture fraction joint pdf $\tilde{f}_{\mathbf{U}\xi}(\mathbf{V}, \hat{\xi}; x, r)$,

$$\tilde{f}_{\mathbf{U}\xi\chi}(\mathbf{V}, \hat{\xi}, \hat{\chi}; x, r) = \tilde{f}_{\mathbf{U}\xi}(\mathbf{V}, \hat{\xi}; x, r) \cdot \tilde{f}_{\chi}(\hat{\chi}; x, r). \quad (12)$$

For the velocity-mixture fraction pdf, stochastic mixing models simulate molecular diffusion and a stochastic re-orientation model accounts for the fluctuating pressure gradient.¹² Intermittency is included using conditional models developed by Pope.^{12,16} Since the pdf being considered is a one-point statistical quantity, some kind of scale information must be supplied. A turbulent frequency ω is defined in terms of the (density-weighted) turbulent kinetic energy \bar{k} and its viscous dissipation rate $\bar{\epsilon}$, $\omega(x, r) \equiv \bar{\epsilon}/\bar{k}$. It is assumed that ω is uniform across the flow; the value of the turbulent frequency is taken to be proportional to a mean flow inverse time scale.^{7,16} In the present study, the values of all model constants are identical to those used in previous calculations of this flow.^{7,16}

The modeling of the scalar dissipation pdf has been discussed in detail elsewhere.^{4,5,6,7} It is assumed that \tilde{f}_{χ} is a log-normal distribution; that is, the density-weighted pdf of the natural logarithm of χ is a Gaussian distribution with mean $\mu(x, r)$ and variance $\sigma^2(x, r)$. The parameters μ and σ^2 are related to the density-weighted mean and variance of χ by

$$\bar{\chi}(x, r) = \exp\{\mu(x, r) + \sigma^2(x, r)/2\}, \quad (13)$$

and

$$\widetilde{\chi''^2}(x, r) = \bar{\chi}^2(x, r)[\exp\{\sigma^2(x, r)\} - 1]. \quad (14)$$

Then $\mu(x, r)$ and $\sigma^2(x, r)$ must be specified as functions of local mean quantities. For the mean, we adopt the usual modeling assumption relating the mean scalar dissipation to the density-weighted mixture fraction variance $\bar{\xi}''^2$,

$$\tilde{\chi} = C_\phi \omega \tilde{\xi}''^2, \quad (15)$$

where the value of the model constant is $C_\phi = 2$. The variance σ^2 is taken to be proportional to the local intermittency factor $\tilde{\gamma}(x, r)$,

$$\sigma^2(x, r) = 1.0\tilde{\gamma}(x, r). \quad (16)$$

Here $\tilde{\gamma}$ is the probability of the flow being turbulent at position (x, r) : $\tilde{\gamma}(x, 0) = 1$, and $\tilde{\gamma}(x, r \rightarrow \infty) = 0$.

Numerical Solution Algorithm

Because of the large dimensionality of the joint pdf $\tilde{f}_{U\xi\chi}$, a Monte Carlo solution algorithm is adopted. The pdf is represented by a large number N of notional particles ($N \approx 100,000$ in the present calculations). Each particle exists in the seven-dimensional position-velocity-composition state space. The number density of particles in velocity-composition space at a fixed physical position represents the local density-weighted joint pdf.¹²

The solution is obtained by marching the notional particles in the x direction by an amount Δx in each computational step. The corresponding time step for the n th particle is $\Delta t^{(n)} = \Delta x/U^{(n)}$, $n = 1, \dots, N$. To apply the transient flamelet model, we keep track of the total time-of-flight or residence time for each particle. The time-of-flight for the n th particle after m time steps is

$$t^{(n)} = \sum_{j=1}^m \Delta t_j^{(n)}. \quad (17)$$

The minimum allowable stretch for the particle is then $\alpha_{\min} = A(t^{(n)})$, Eq. (10). For a laminar flamelet, this α_{\min} corresponds to a scalar dissipation χ_{\min} .

On each step, particle positions, velocities, and mixture fraction evolve by the models described earlier. The particle scalar dissipation is selected from a log-normal distribution whose parameters are related to the local one-point flow statistics according to Eqs. (13)–(16). The density, temperature, or any other thermochemical property associated with a particle is determined by a two-dimensional (ξ and χ) table lookup in the laminar flamelet library using linear interpolation. For $\chi^{(n)} > \chi_q$, the maximum tabulated value $\chi^{(n)} = \chi_q$ is used; it has been verified that this event occurs rarely in the present flow.⁷ For $\chi^{(n)} < \chi_{\min}$, the minimum allowable value $\chi^{(n)} = \chi_{\min}$ is used. Mean quantities are evaluated using an ensemble averaging and spline-smoothing procedure.^{7,12}

The calculations are started at the nozzle exit $x/D = 0$ with $A_0 = \alpha_q = 4800/s$ (Eq. 10), the extinction limit. The downstream results are not sen-

sitive to this choice of A_0 : for large t , Eq. (10) gives $A(t) \rightarrow .5(t - t_0)^{-1}$. Measured initial profiles of mean velocity and turbulence quantities are not matched in detail, but the momentum and mixture fraction fluxes are set to the experimental values. Approximately 950 steps are taken to march the solution downstream to $x/D = 100$.

The only difference between the present calculations and those reported by Haworth et al.⁷ is the truncation of flamelets with $\chi < \chi_{\min}$ to account for the finite response time of laminar flamelets to changes in the turbulent flow field.

Results and Discussion

In this section we concentrate on the differences between the present results and those reported earlier⁷ based on the standard flamelet model. These differences may best be understood by an examination of the evolution of the pdf of scalar dissipation. In the standard flamelet model (SF), the pdf of scalar dissipation in the turbulent flow $\tilde{f}_\chi(\tilde{\chi}; x, r)$ is the same as the pdf of quasi-steady flamelet structures or effective flamelet stretch $\tilde{g}_\chi(\tilde{\chi}; x, r)$. In the modified flamelet model (MF), the pdf of scalar dissipation remains the same while the pdf of equivalent quasi-steady flamelet structures needs to be modified by truncating all samples with $\chi^{(n)} < \chi_{\min}$ and replacing them with a sample at χ_{\min} . It is emphasized that in the modified model, \tilde{g}_χ is not to be interpreted as the scalar dissipation in the turbulent flow but only as the pdf for the selection of flamelets from the laminar flame library. In the Monte Carlo calculations, the truncation is based on the time-of-flight of each notional particle (Eq. 17); thus χ_{\min} is itself a random variable. For illustrative purposes, we consider a mean time-of-flight $\bar{t}(x)$ based on the mean flow velocity at the location of the mean stoichiometric mixture fraction in the turbulent flame,

$$\bar{t}(x) \equiv \int_0^x \bar{U}^{-1}(x', r_{St}) dx', \quad (18)$$

where $\tilde{\xi}(x, r_{St}) = \xi_{St}$. For x such that $\tilde{\xi}(x, 0) < \xi_{St}$, we take $r_{St} = 0$.

Figure 1 shows $\tilde{f}_\chi(\tilde{\chi}; x, r_{St})$ and $\tilde{g}_\chi(\tilde{\chi}; x, r_{St})$, the latter based on $\alpha_{\min} = A(\bar{t}(x))$ (Eq. 10), at three streamwise locations. The pdf \tilde{f}_χ is log-normal in all cases. At the nozzle, \tilde{g}_χ is a delta function at $\tilde{\chi} = \chi_q$; as we move downstream, the distribution \tilde{g}_χ at first broadens as χ_{\min} decays; then for larger x/D , χ_{\min} decreases as $(x/D)^{-1}$ while $\tilde{\chi}$ scales as $(x/D)^{-4}$, so that \tilde{g}_χ narrows to a delta function at $\tilde{\chi} = \chi_{\min}$. Truncation based on actual particle times-of-flight tends to broaden the delta functions.

These trends are viewed in a different way in

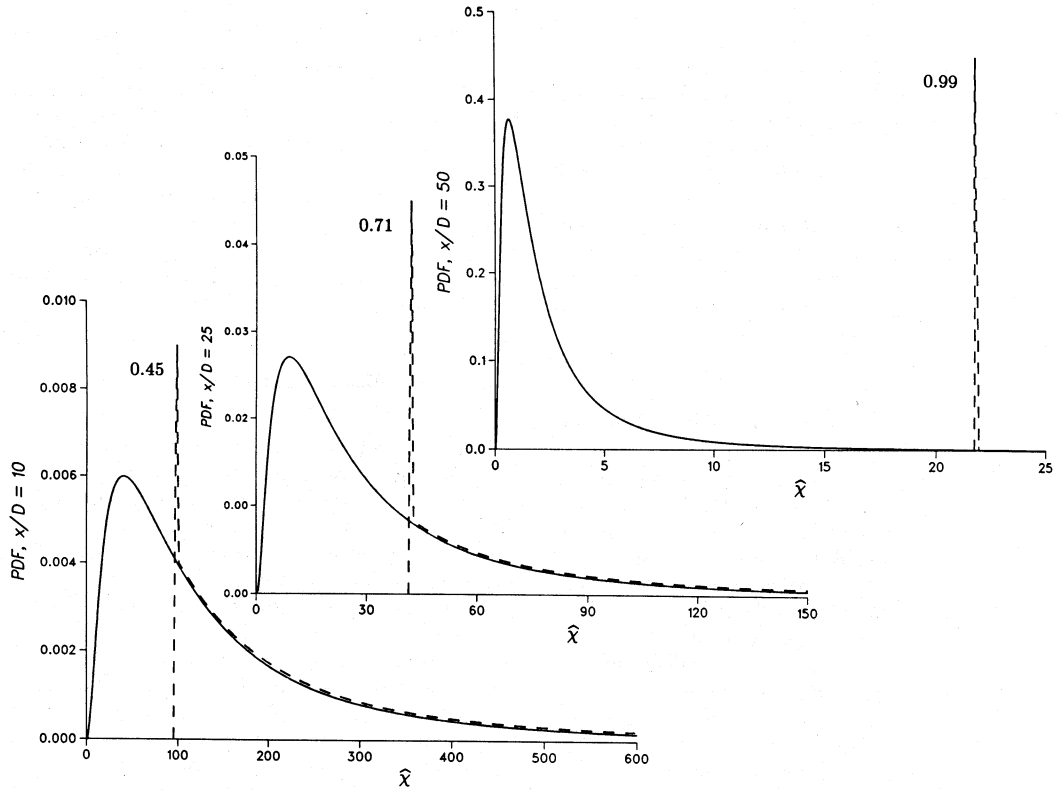


FIG. 1. Pdf's of scalar dissipation $\tilde{f}_\chi(\hat{\chi}; x, r_{st})$, —, and pdf's of quasi-steady flamelet structures $\tilde{g}_\chi(\hat{\chi}; x, r_{st})$, ----, at three axial stations. Spikes correspond to delta functions at $\hat{\chi} = \chi_{\min}$ with magnitudes as shown. For $\hat{\chi} > \chi_{\min}$, the two pdf's coincide.

Fig. 2. Here the evolution of the mean scalar dissipation on the jet centerline and of the peak mean scalar dissipation are shown as functions of x/D . It may be seen that the peak mean scalar dissipation at first increases with x/D to about $x/D = 1$; it then decays as $(x/D)^{-1}$ up to $x/D \approx 10$; and finally, it asymptotes to the $(x/D)^{-4}$ decay law characteristic of a self-similar axisymmetric free jet. Also shown in Fig. 2 is the evolution of χ_{\min} based on $\tilde{i}(x)$. The effect of the truncation of flamelets with $\chi < \chi_{\min}$ is to slow the approach to chemical equilibrium from $(x/D)^{-4}$ in the standard flamelet model to $(x/D)^{-1}$ in the modified model.

Next we examine calculated mean profiles from the flamelet models. The principal discrepancy between the standard model and experiment is the overly rapid approach to equilibrium OH levels given by the model.⁷ Here mean and rms OH concentrations from the SF and MF models are compared with experimental data at two axial stations, $x/D = 25$ and $x/D = 50$. Also shown are results based on a partial equilibrium chemistry model and velocity-composition joint pdf turbulence closure

(PE).¹⁶ At $x/D = 10$ (not shown), the modified flamelet model results are indistinguishable from those of the standard model.

Results at $x/D = 25$ are presented in Figs. 3 and 4. Mean OH levels based on major species concentrations and an equilibrium assumption are shown in Fig. 3; actual measured values are up to five times higher. Here the peak mean OH levels from MF show a modest improvement over SF, while the centerline values from the two models are about the same. The MF rms curve is altered only slightly with respect to the standard model curve (Fig. 4). For both mean and rms, the flamelet models show better agreement with experiment in the vicinity of the jet centerline than does the partial equilibrium model. All three models show substantial superequilibrium OH. Since the reported measurement uncertainty in absolute OH measurements is $\pm 30\%$,⁹ the differences in peak values among the three models in Figs. 3 and 4 provide little basis for selecting one model over the others. Their behavior near the centerline is more revealing.

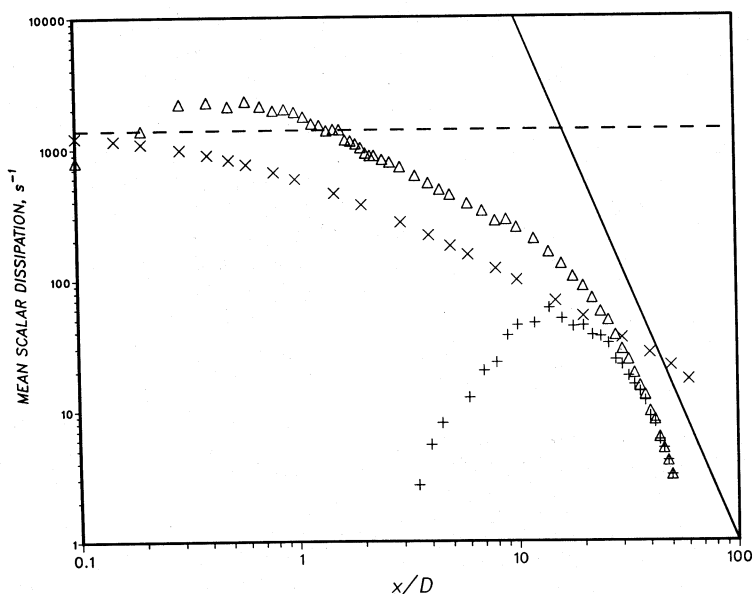


FIG. 2. Streamwise evolution of the mean scalar dissipation on jet centerline (+), of the peak mean scalar dissipation (Δ), and of the truncation limit χ_{\min} based on mean time-of-flight (\times). The streamwise coordinate x is normalized by the nozzle diameter D . Solid line is a reference line with slope -4 ; dashed line corresponds to the extinction limit $\chi_q = 1380/s$.

We now move downstream to $x/D = 50$. Here the differences between MF and SF are more dramatic. Modified flamelet model mean OH concentrations show substantially higher departures from equilibrium than the SF model (Fig. 5) and are comparable to the PE results. Rms values from the

modified model (Fig. 6) also show a small improvement. Mean temperatures (not shown) from MF are slightly lower than those from SF, consistent with the more marked departure from chemical equilibrium of the former model at this station.

Conclusion

An ad hoc approach to incorporating time-dependent flame structures into a laminar flamelet

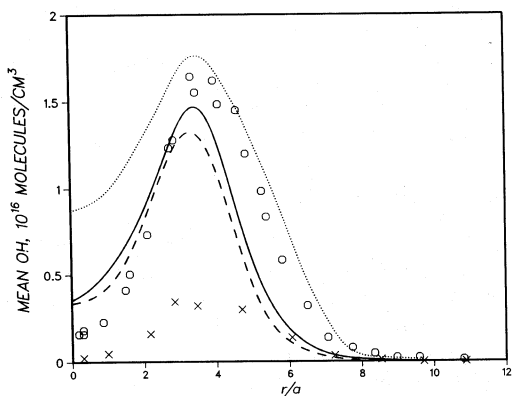


FIG. 3. Profiles of mean OH concentration at $x/D = 25$. The radial coordinate r is normalized by the nozzle radius $a \equiv D/2$. Open symbols are experimental data,⁹ crosses are equilibrium OH based on major species measurements,⁹ lines are calculations: —, modified flamelet (MF); - - - standard flamelet⁷ (SF); ···· partial equilibrium¹⁶ (PE).

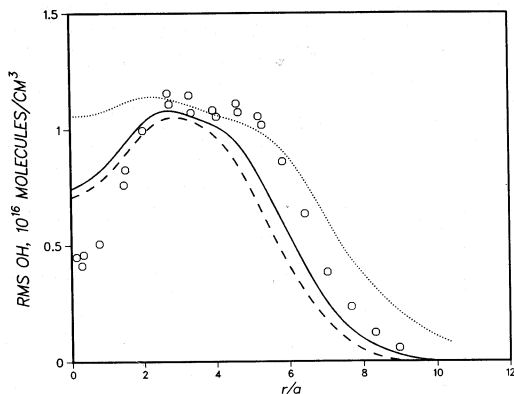


FIG. 4. Profiles of rms OH concentration at $x/D = 25$. Lines and symbols are the same as in Fig. 3.

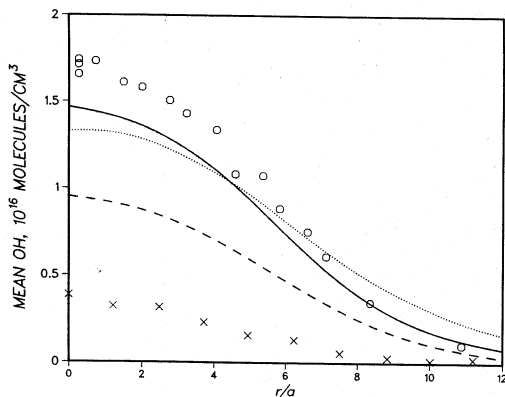


FIG. 5. Profiles of mean OH concentration at $x/D = 50$. Lines and symbols are the same as in Fig. 3.

model for turbulent diffusion flames has been presented. The basis for the modified model is the equivalent strain analysis. This analysis suggests that steady-state laminar flame structures cannot exist far downstream in the flow. In the modified flamelet model, we continue to use a steady-state flamelet library but flames are selected from the library in a way that accounts for the residence time limit on the growth of diffusive layers in the jet. The modified flamelet model results in a slower approach to chemical equilibrium in closer agreement with experiment than the standard model. The level of agreement between modified flamelet model and experiment is comparable to that of a two-scalar partial equilibrium scheme.¹⁶ Thus in turbulent jet diffusion flames, transient flamelet effects may be more important than previously assumed. In turbulent nonpremixed flames where the mean scalar dissipation does not evolve as rapidly, transient effects may be less important. Work is in progress to compare quantitatively the calculated transient re-

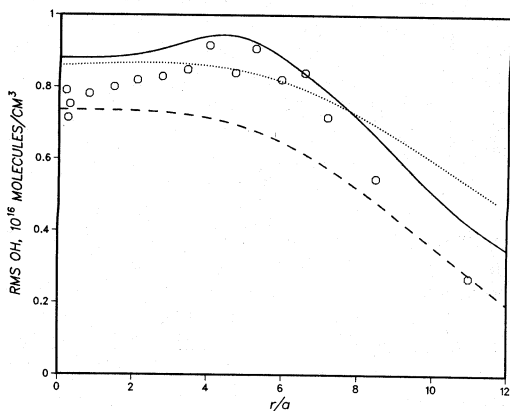


FIG. 6. Profiles of rms OH concentration at $x/D = 50$. Lines and symbols are the same as in Fig. 3.

sponse of stretched opposed-flow laminar diffusion flames to the equivalent strain model.

REFERENCES

1. CARRIER, G. F., FENDELL, F. E. AND MARBLE, F. E.: *SIAM J. Appl. Math.* 28, 463 (1975).
2. WILLIAMS, F. A.: *Turbulent Mixing in Non-reactive and Reactive Flows* (S. N. B. Murthy, Ed.), p. 189, Plenum Press, 1975.
3. PETERS, N.: *Prog. Energy Comb. Sci.* 10, 319 (1984).
4. LIEW, S. K., BRAY, K. N. C. AND MOSS, J. B.: *Comb. Flame* 56, 199 (1984).
5. ROGG, B., BEHRENDT, F. AND WARNATZ, J.: *Twenty-First Symposium (International) on Combustion*, p. 1533, The Combustion Institute, 1988.
6. BEHRENDT, F., BOCKHORN, H., ROGG, B. AND WARNATZ, J.: "Modeling of turbulent CO/air diffusion flames with detailed chemistry," *Proc. 2nd International Workshop on Modeling of Chemical Reaction Systems* (J. Warnatz, Ed.), Springer, 1986 (in press).
7. HAWORTH, D. C., DRAKE, M. C. AND BLINT, R. J.: "Stretched laminar flamelet modeling of a turbulent jet diffusion flame," *GMR Research Publication No. GMR-6023*, Nov. 1987 (accepted for publication in *Comb. Sci. Tech.*).
8. DRAKE, M. C., PITZ, R. W., CORREA, S. M. AND LAPP, M.: *Twentieth Symposium (International) on Combustion*, p. 1983, The Combustion Institute, 1985.
9. CORREA, S. M., DRAKE, M. C., PITZ, R. W. AND SHYY, W.: *Twentieth Symposium (International) on Combustion*, p. 338, The Combustion Institute, 1985.
10. DRAKE, M. C.: *Twenty-First Symposium (International) on Combustion*, p. 1579, The Combustion Institute, 1988.
11. SAITOH, T. AND OTSUKA, Y.: *Comb. Sci. Tech.* 12, 135 (1976).
12. POPE, S. B.: *Prog. Energy Comb. Sci.* 11, 119 (1985).
13. DRAKE, M. C. AND BLINT, R. J.: "Thermal NO_x in stretched laminar opposed-flow diffusion flames with $\text{CO}/\text{H}_2/\text{N}_2$ fuel," *GMR Research Publication No. GMR-5800*, May 1987 (submitted for publication).
14. DRAKE, M. C. AND BLINT, R. J.: "Structure of laminar opposed-flow diffusion flames with $\text{CO}/\text{H}_2/\text{N}_2$ fuel," *GMR Research Publication No. GMR-6103*, Dec. 1987 (accepted for publication in *Comb. Sci. Tech.*).
15. TENNEKES, H. AND LUMLEY, J. L.: *A First Course in Turbulence*, MIT, 1972.
16. POPE, S. B. AND CORREA, S. M.: *Twenty-First Symposium (International) on Combustion*, p. 1341, The Combustion Institute, 1988.

COMMENTS

M. A. Delichatsios, Factory Mutual Research, USA. I have two questions: 1) Are there any experiments wherein the chemical structure of a laminar flame has been measured for transient straining rates? How do they compare with your assumed transient response model? 2) Is it true that the effects of straining rates in your turbulent model are only limited to the effects of large scale straining rates but not Kolmogorov straining rates? How could you incorporate those (Kolmogorov) effects?

Author's Reply. There are, to our knowledge, no experimental data available for the detailed time-dependent chemical structure of strained laminar diffusion flames. Saitoh and Otsuka (Ref. 11 of paper) studied the global response of opposed-flow laminar diffusion flames to time-varying strains; their results show that the time response is inversely related to the strain rate, which is in qualitative agreement with the analysis in this paper. It is our intention to investigate numerically the time-dependent laminar flame structure for an opposed-flow stagnation point burner configuration including detailed kinetics. Preliminary calculations confirm the analysis, provided that the rate-of-change of strain rate is not too large.

Straining at all scales is accounted for in the one-dimensional transient diffusion layer analysis, as long as the diffusive layer is thin compared to the smallest turbulent straining scales. The residence time implementation in the turbulent jet does not contain complete details of the strain history following a flamelet. An advantage of the Monte Carlo approach, which follows notional particles through the flow field, is that if we knew the actual strain history $a(t)$ (including all relevant scales) then Eq. (9) could be integrated directly to yield $A(t)$.

N. Peters, RWTH, Fed. Rep. of Germany. You relate the variance of the scalar dissipation rate to the intermittency factor. What is the physical basis for this modeling assumption?

Author's Reply. The assumed proportionality between σ^2 and $\bar{\gamma}$ (Eq. 16) is based on empirical evi-

dence rather than on physical arguments. Measurements by Namazian et al.¹ in a nonreacting methane-air jet show that σ is nearly uniform across the turbulent core of the jet, and that σ decreases at the outer edge of the jet; this same behavior is exhibited by the intermittency factor $\bar{\gamma}$. Results in the turbulent jet flame change little if we simply take $\sigma^2 = 1$ everywhere.

REFERENCE

1. NAMAZIAN, M. SCHEFER, R. W., AND KELLY, J.: "Scalar dissipation measurements in the developing region of a jet," Sandia National Laboratories Report No. SAND87-8652, November 1987 (submitted for publication).

W. A. Sirignano, Univ. of California/Irvine, USA. Equation (2) is not correct in the variable density case. In particular, the strain rate cannot be represented as dependent only on time and independent of spatial position. The strain rate is related to a time derivative of density when the velocity divergence is non-zero. That density derivative is dependent both on space and time.

Author's Reply. The uniform property one-dimensional strained transient diffusive layer of the model differs from a strained laminar diffusion flame in several respects: the latter includes effects such as chemical reaction, differential diffusion, and spatial gradients of density and diffusivity. Clearly the model breaks down if these effects become dominant. Peters (Ref. 3 of paper) argues that the temperature dependence of diffusivity and of density tend to cancel one another, so the χ vs. ξ relationship is nearly the same as in the constant temperature diffusive layer. Time-dependent detailed chemistry calculations for laminar flames in an opposed-flow stagnation point burner are being performed to quantify the limits of applicability of the simple model.